Supporting information for

Room-temperature Large Magnetic-dielectric Coupling in New Phased Anatase $VTiO_4$

Feng Feng[a], Shuanglin Hu[b], Yuqiao Guo[a], Jiyin Zhao[a], Ngai Yui Chan[c], Linfeng Fei[c], Wensheng Yan[a], Wei Ning[d], Jinlong Yang[a], Yu Wang[c] and Yi Xie[a], Changzheng Wu[a*†]

a Hefei National Laboratory for Physical Sciences at the Microscale & National Synchrotron Radiation Laboratory, University of Science and Technology of China, Hefei, Anhui, 230026, P. R. China.

b Department of Chemistry, The Ångström Laboratory, Uppsala University, Box 538, SE-75121 Uppsala, Sweden.

c Department of Applied Physics and Material Research Center, The Hong Kong Polytechnic University, Hong Kong SAR, P. R. China.

d High Magnetic Field Laboratory, Chinese Academy of Sciences, Hefei 230031, Anhui Province, P. R. China.

Email: czwu@ustc.edu.cn; Fax: 86-551-63606266.

Table of contents

S1. Experimental Section

1. *Synthesizing of anatase $VTiO_4$, $V_{0.4}Ti_{1.6}O_4$ and $V_{0.2}Ti_{1.8}O_4$ nanocystal*

Anatase $VTiO_4$ nanoparticles were prepared by a simple hydrothermal process. In a typical procedure of synthesizing the anatase $VTiO_4$, 1.0 mmol vanadium(IV)oxy acetylacetonate ($VO(acac)_2$) and 0.55 mmol dipotassium titanium oxide dioxalate ($K_2TiO(C_2O_4)_2$) were dissolved into 40 mL distilled water in a glass beaker, which was stirred for 30 minutes forming a green homogeneous solution, and then transferred into a 50 mL Teflon-lined autoclave. The autoclave was sealed and heated at 200 ^{o}C for 10 h. The system was allowed to cool to room temperature. Finally, the dark green product was collected by centrifugation and washed with deionized water and ethanol for several times to remove any ionic and organic remnants, then dried in vacuum at 60 ^{o}C.

For the synthesis of $V_{0.4}Ti_{1.6}O_4$ (named as V1T4) and $V_{0.2}Ti_{1.8}O_4$ (named as V1T9), the adding amounts of $K_2TiO(C_2O_4)_2$ has changed to 1.0 and 1.5 mmol, respectively, while maintaining the other experimental conditions. The formation of $V_{0.4}Ti_{1.6}O_4$ and $V_{0.2}Ti_{1.8}O_4$ in anatase structure has been verified by the XRD pattern. ICP-AES measured the element content of the as-obtained two samples accurately, revealing that the weight percent of V and Ti were 26.74 w%: 7.24 w% and 30.99 w%: 3.65 w%, in which the V/Ti molar ratio were approaching to 1:4 and 1:9.

2. *Characterizations*

The as-prepared samples were characterized by X-ray powder diffraction (XRD) with a Philips X'Pert Pro Super diffractometer with Cu Kα radiation (λ =1.54178 Å). The HRTEM image and energy dispersive X-ray spectroscopy (EDS) were obtained on a JEOL-2010 transmission electron microscope at an acceleration voltage of 220 kV. Transmission electron microscopy (TEM), scanning transmission electron microscopy (STEM) images and energy dispersive X-ray spectrums (EDS) were obtained on a JEM 2100F (field emission) transmission electron microscopes equipped with an Oxford INCA x-sight EDS Si(Li) detector at an acceleration voltage of 200 kV. The near edge X-ray absorption spectra were measured at the U19 beamline of the National Synchrotron Radiation Laboratory, with temperature controlling equipment.

The magnetic measurements were carried out with a superconducting quantum interference device magnetometer (Quantum Design MPMS XL-7). The temperature dependent dc magnetization of the compound was measured on warming with a magnetic field of H=1000 Oe.

For the measurement of dielectric property and magneodielectricity, the $VTiO_4$ nanoparticles were first pressed into a pellet with diameter of 12mm and the thickness of 0.77mm. Au electrodes were then deposited onto the opposite faces of the pellets.

The samples were placed in Linkam THMS 94 probe station which provided the varying temperature environment from 100 K to 350 K. Dielectric properties were determined using Agilent 4294A precision impedance analyzer (Malaysia) at various frequencies (100 Hz – 1 MHz). Standard calibrations under open and short-circuit conditions were performed prior to all capacitance measurements to remove features in measured capacitance associated with the connecting cables and the background circuit. For the measuring of magnetodielectric response, the sample pellet with electrodes was put onto the holder of LakeShore 7600 Vibrating Sample Magnetometry (VSM) system. Magnetic field was applied through VSM system and the corresponding capacitance was measured by Stanford SR720 LCR Meter.

S2 STEM and HRTEM images of $V_{0.4}Ti_{1.6}O_4$ and $V_{0.2}Ti_{1.8}O_4$

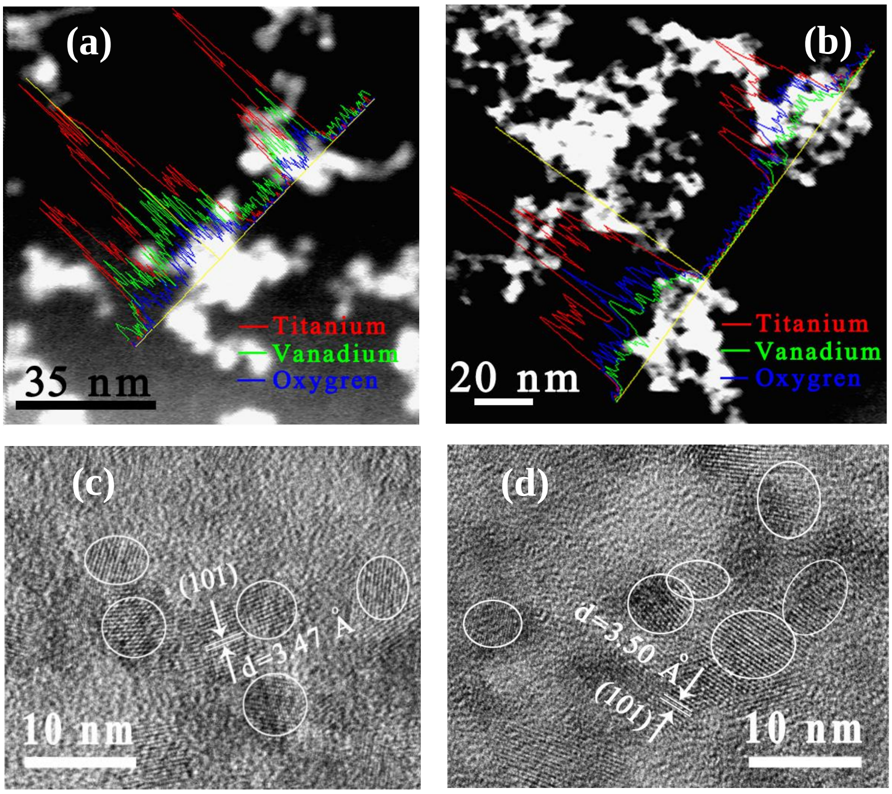

Figure S1 The STEM images of $V_{0.4}Ti_{1.6}O_4$ (a) and $V_{0.2}Ti_{1.8}O_4$ (b), in which the fluctuation of V and Ti elemental content were consistent, showed the homogeneous distribution of V and Ti in samples. The HRTEM images of $V_{0.4}Ti_{1.6}O_4$ (c) and $V_{0.2}Ti_{1.8}O_4$ (d) gave the morphology and microstructure. Both of $V_{0.4}Ti_{1.6}O_4$ and $V_{0.2}Ti_{1.8}O_4$ were in nanocrystal outlook with particle size of 5~9 nm. Moreover, the interplanar spacing of these two products were 3.47 Å and 3.50 Å, respectively, both of which were a slightly less than the d value of (101) plane (d=3.5167 Å) for pure anatase structure, in accordance of d value with that from the lattice plane distance from XRD pattern, verifying the anatase structure of $V_{0.4}Ti_{1.6}O_4$ and $V_{0.2}Ti_{1.8}O_4$

further.

S3. Partial XRD pattern of anatase $VTiO_4$, $V_{0.4}Ti_{1.6}O_4$ (V1T4) and $V_{0.2}Ti_{1.8}O_4$ (V1T9) nanocystal

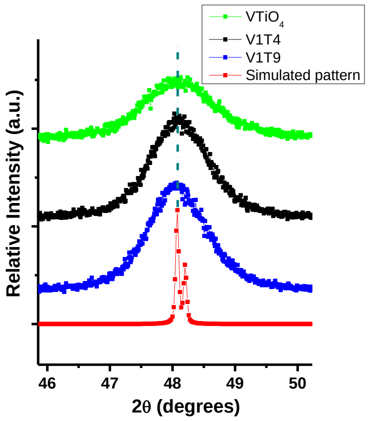

Figure S2 Partial XRD patterns of $VTiO_4$, V1T4, V1T9 and simulated curve of (200) peak in the range of $46^o \leq 2\theta \leq 50^o$, in which the dash dot line showed that the position of the (200) peak of the three samples did not shift from the simulated pattern at all.

S4. The relationship of lattice parameter and unit cell volume with vanadium content

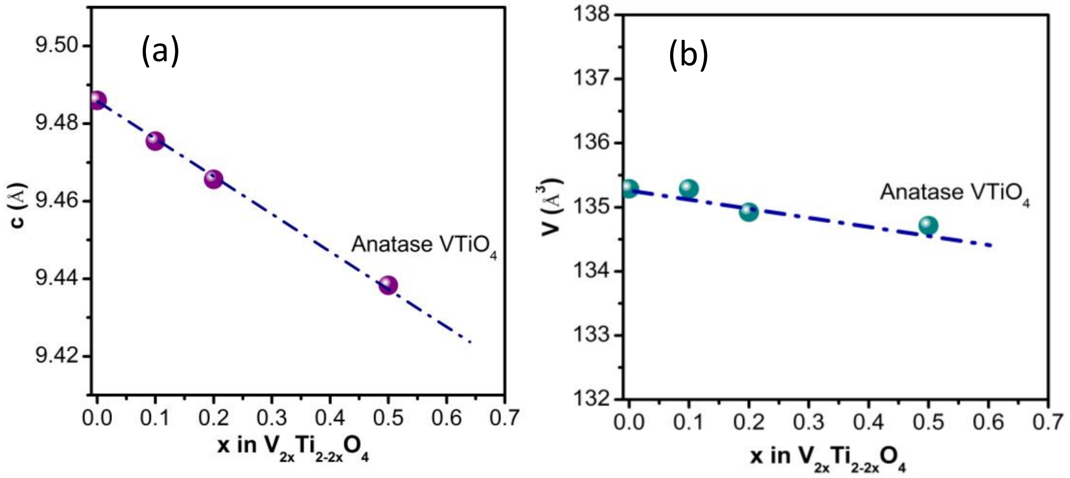

Figure S3 The lattice parameter c (a) and cell volume (b) decrease with the increasing of V content in anatase TiO_2 linearly, both of which obey Vergard's law.

S5. XAS spectroscopy of anatase $VTiO_4$, $V_{0.4}Ti_{1.6}O_4$ (V1T4) and $V_{0.2}Ti_{1.8}O_4$ (V1T9)

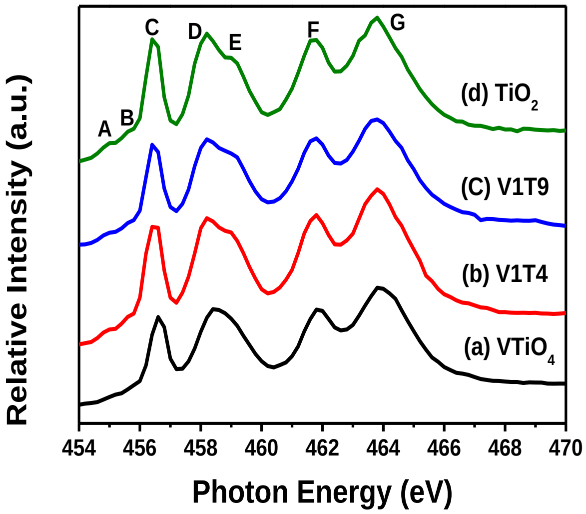

Figure S4 L-edge of Ti XAS spectra of (a) $VTiO_4$, (b) V1T4, (c) V1T9 and (d) pure anatase TiO_2. In the spectra, the well defined peak C results from the transition from Ti $2p_{1/2}$ to t_{2g} state, peak D and E originates from the transition from Ti $2p_{1/2}$ to e_g state, peak F is assigned to transition from Ti $2p_{3/2}$ to t_{2g} state and peak G is relate to transition from Ti $2p_{3/2}$ to e_g state [1].

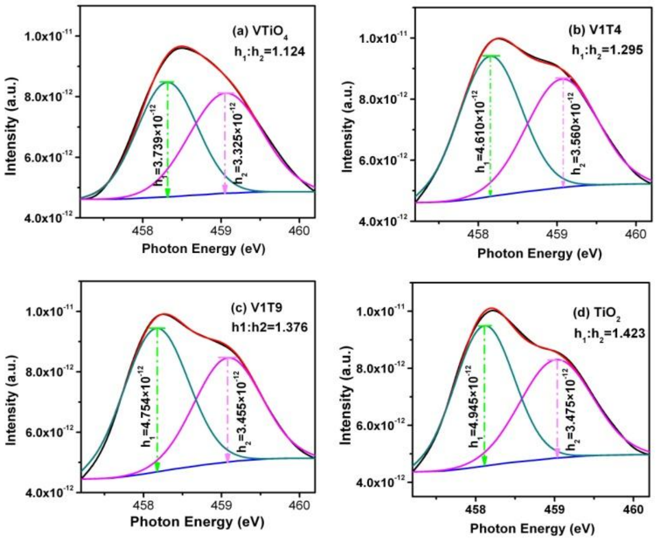

Figure S5 The partial enlarged details of D, E peak in XAS spectra of Ti L-edge for the four anatase samples (a) $VTiO_4$, (b) V1T4, (c) V1T9 and (d) pure anatase TiO_2

S6. Observation of the size distributions for anatase $VTiO_4$ nanocrystal

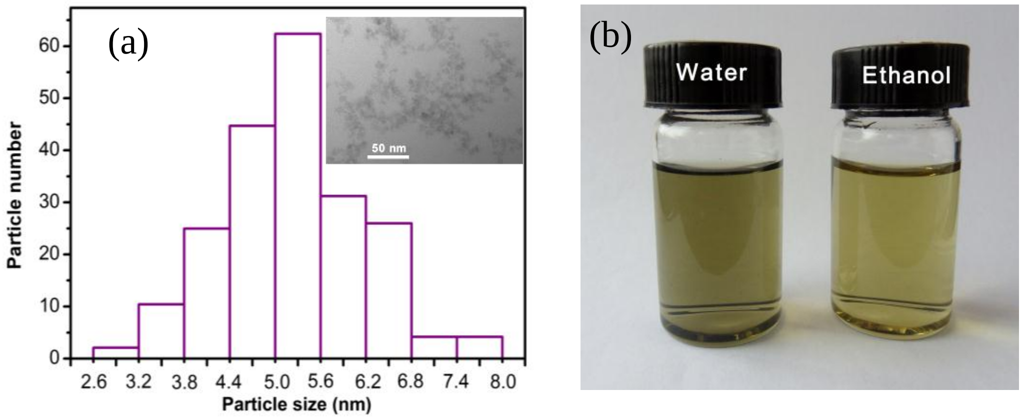

Figure S6 (a) Size distribution of anatase $VTiO_4$ nanocrystals and the inset is TEM image, which reveal the size of nanoperticles obey the normal distribution, representing the anatase $VTiO_4$ was nanoparticles with size ranging from 2 to 8 nm.. (b) Digital images of the anatase $VTiO_4$ nanocrystal dispersions in water (left) and ethanol (right), forming a transparent yellowish green system. And it would not precipitate even over two months.

S7. EDS spectroscopy of anatase $VTiO_4$

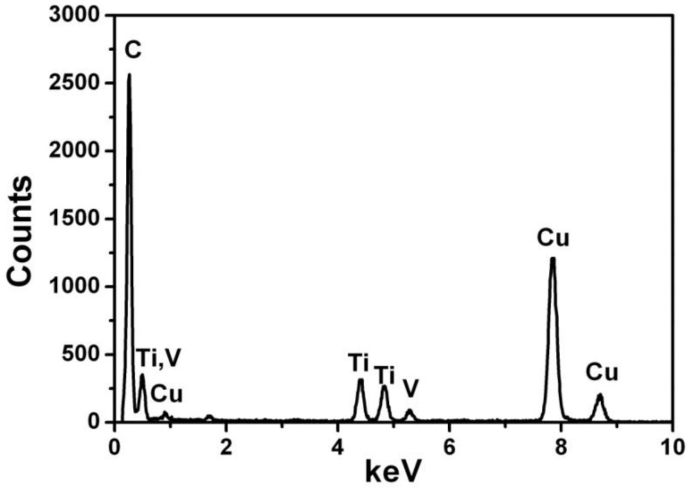

Figure S7 EDS spectrum of the anatase $VTiO_4$ sample analyzed the type and contents of elements in the sample. Obviously, there was no other elements contained in the sample except for vanadium, titanium and oxygen (C and Cu were derived from cooper grids) and atom percent of V and Ti were 13.53% and 16.97%, considering the systematic error, the ratio of V/Ti was approaching 1:1.

S8. Magnetic measurement of anatase $VTiO_4$

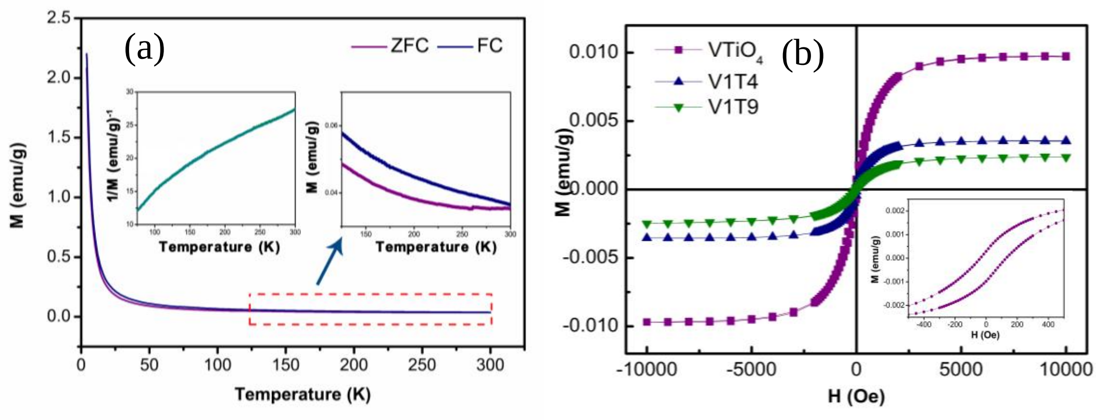

Figure S8 (a) ZFC and FC curve of measured in the field of 100 Oe from 4 to 300K. The left inset curve is the inverse magnetization of ZFC versus temperature and the right one is the enlarger ZFC and FC curve from 125 to 300 K. (b) M-H curve of anatase $VTiO_4$, V1T4 and V1T9 at 300 K within 10000 Oe. The inset is the enlarged M-H curve of anatase $VTiO_4$ at 300 K in low field.

All the M-H, ZFC and FC experimental data has proven the ferromagnetic behavior of anatase $VTiO_4$. The ZFC and FC curve (**Figure S8a**) measured under 100 Oe separated with each other giving the proof of non-paramagnetic property. In addition, the absence of typical freezing point of superparamagnetism in the ZFC curve proved that our anatase $VTiO_4$ nanoparticle was not superparamagnetic. Furthermore, the inverse magnetization versus temperature curve did not obey linear Curie-Weiss law, as shown in the left inset of **Figure S8a**, meaning that the anatase $VTiO_4$ was not paramagnetic also. Moreover, the M-H curve measured at 300 K exhibits a clear hysteresis loop, which offers a solid evidence to demonstrate the ferromagnetic property of anatase $VTiO_4$. In the M-H curve (**Figure S8b**) measured at 300 K between -10000 and 10000 Oe, the saturation magnetization (M_s) value of anatase $VTiO_4$ is 0.01 emu/g. And the enlarged M(H) curves in the low-field region (**Figure S8b insets**) showed that the coercivity of anatase $VTiO_4$ was about 128 Oe. **Figure S8b** also displayed that the value of saturation magnetization increased with vanadium contents rising, indicating incorporated V^{4+} ions were responsible for the room temperature ferromagnetic property. In summary, magnetical characterizations of M-H, ZFC and FC have further confirmed the room-temperature ferromagnetism of anatase $VTiO_4$.

S9. Calculation detail for the new-phased anatase $VTiO_4$ structure

The geometric, electronic, and magnetic structure of anatase TiO_2 and anatase $VTiO_4$ were calculated using the projector augmented-wave (PAW) method[2] with the Perdew-Burke-Ernzerhof (PBE) generalized gradient approximation (GGA) functional[3] and GGA+U as implemented in VASP code[4]. The energy cutoff was set to 500 eV. Gamma-centered Monkhorst-Pack k-points sampling method with 9×9×3 and 14×14×6 were used for geometry relaxation and total energy calculations of unit cell, respectively. The geometries were relaxed until residual atomic forces less than 0.01eV/Å, and then the total energies were calculated converged to 10-5 eV per unit cell.

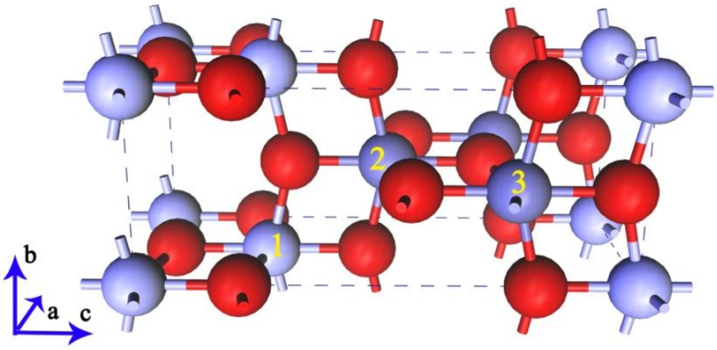

Figure S9 The geometry structure of anatase TiO_2 (The purple and red balls represent Ti and O atoms, respectively)

Our model of anatase TiO_2 adopted 4 Ti atoms and 8 O atoms in one cell, the lattice parameter is a=b=3.807Å and c=9.725Å. The geometry configuration is presented in Fig. 1, and then we checked its electronic properties. The anatase TiO_2 was calculated to be a nonmagnetic semiconductor with a band gap of 2.05eV. It is lower than the experimental 3eV[5,6], but is close to other DFT calculation results.[7] The well known underestimation of band gap within DFT is due to insufficient cancellation of the self-interaction energy. However, since we are comparing the properties of TiO_2 with and without V doping, the absolute band gap value is less important than the gap varying trends.

There are two configurations for anatase $VTiO_4$ that is the nearest neighbouring (NN) and the next neighbouring (NNN) configuration. To be clearly, we note the Ti atom in **Figure S9**. When Ti1 and Ti2 are replaced by V, which is NN configuration. If Ti1 and Ti3 are replaced by V, the NNN configuration forms. And for each configuration, two V atoms can further couple with ferromagnetic (FM) or anti-ferromagnetic (AFM) order. It is worth noting that the NN replacement of V to Ti reduced the symmetry of anatase and made the lattice parameter *a* different from *b*, while the NNN replacement kept *a* and *b* the same.

We tested all the four configurations, performed geometry relaxation and electronic calculations. The results are presented in Table S1. In this table, ΔE is the Calculated energy difference between the AFM and FM states of nearest neighboring (NN) V doping $VTiO_4$ system [ΔE=E(AFM)-E(FM)], M is the projected magnetic moment (M) on per V atom, E(gap) is energy band gap (E_{gap})for ground state FM-NN configuration, and the last column is the E(AFM)-E(FM) for next nearest neighboring (NNN) V doping configuration, and the values in parenthesis are energy difference of E(FM-NNN)-E(FM-NN).

Table S1. Calculation results of $VTiO_4$ system through PBE+U method

method	ΔE (meV/V atom)	M (μB/V atom)	E(gap) (eV)	ΔE(NNN) (meV/V atom)
PBE	53.5	1.022	0	10.0(146)
PBE+U=3eV	17.0	1.048	0.08	10.8(840)
PBE+U=5eV	12.5	1.066	0.87	-54.8(1569)
PBE+U=7eV	10.5	1.089	1.68	-169.0(2321)

In the model of one unit cell, V^{4+} ions are FM coupling automatically in *a* and *b* direction. We also doubled the unit cell in lattice *a* or *b* direction to check the stability of AFM coupling within the case of U_{eff} = 5eV. After geometry relaxation and total energy calculations, the states started with a initial AFM configuration all tended to become paramagnetic, i.e. to cancel the local magnetic moment, and which energy were much higher than corresponding FM state. Thus the FM state should be the magnetic ground statein the high doped $VTiO_4$ system.

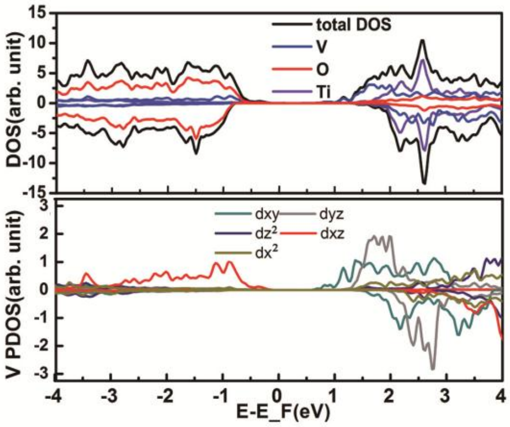

Figure S10 The total and partial density of states (DOS) of $VTiO_4$ and the V3d PDOS calculated with U_{eff} = 5 eV

The total density of states (DOS) and projected DOS (PDOS) on V of the FM-NN state were calculated with U_{eff} = 5 eV, which manifested that the magnetic coupling effect was originated from the interaction between V 3d electrons and O 2p electrons. In **Figure S10**, the majority of the V 3d orbitals are unoccupied, except there is one single electron occupying the $3d_{xz}$ orbital on each V ions. The occupied dxz orbital of two V ions interact with the O atoms in the x-z (a-c) plane, and thus coupled to each other contributing to the total density of $VTiO_4$ (**Figure S10**). Calculation results uncovered that the superexchange mechanism in V-O-V configuration induced ferromagnetic ordering.

S10. Dielectric loss of new-phased anatase $VTiO_4$

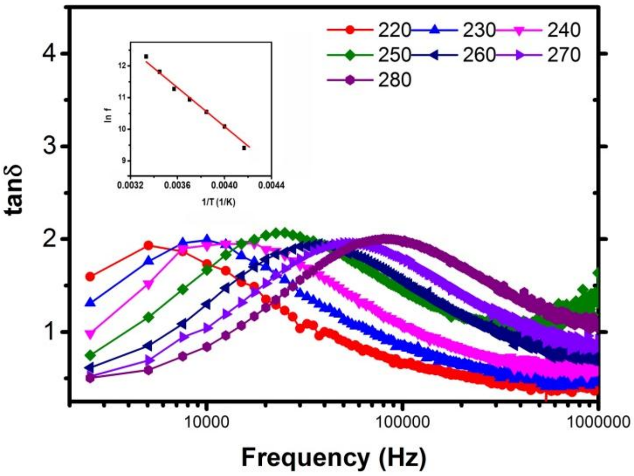

Figure S11 tanδ goes with the frequency (Hz) for $VTiO_4$ at different temperature. In the inserted graph, black points are the frequency value at the position of experimental tanδ peak for every tanδ-frequency curves ranging from 220K to 280K, in which the red line is simulated Arrhenius relation.

To analyze the dielectric relaxation of anatase $VTiO_4$, dielectric loss (tanδ) depending on frequency with temperature increasing was plotted in **Figure S11**. The peak of tanδ corresponded to electric dipoles relaxation. Moreover, the temperature and frequency of electric field obeyed an Arrhenius relation[8,9]:

$$f = f_0 \exp(-Q/kT)$$

where f is the peak frequency in **Figure S11**, f_0 is the prefactor, k is Boltzmann constant, T is the recorded temperature of individual line in **Figure S11** and Q is the activation energy representing the energy needed to reorient each polar region . For this anatase $VTiO_4$ sample, the experimental data points and fitted line from the above equation was presented in **Figure S11**, from which the calculation results was Q= 0.26 eV and f_0= 5.14×10. The Q value of our anatase $VTiO_4$ sample was close to that of nicklate ceramics (Q=0.29 meV) and has been interpreted as the dipole polarization with the activation of local charge centers[10].

Reference

1. Soriano, L.; Ahonen, P. P.; Kauppinen, E. I.; Gómez-García, J; Morant, C; Palomares, F. J.; Sánchez-Agudo, M.; Bressler, P. R.; Sanz, J. M. *Monatshefte für Chemie*. **2002**, 133, 849

2. Blöch, P. E. *Phys. Rev. B* **1994**, 50, 17953.

3. Perdew, J. P.; Burke, K.; Ernzerhof, M. *Phys. Rev. Lett.* **1996**, 77, 3865.

4. (a) Kresse, G.; Hafner, J. *Phys. Rev. B* 1993, 48, 13115; (b) Kresse, G.; Furthmüller, *J. Phys. Rev. B* 1996, 54, 11169; (c) Kresse, G. and Joubert, D. *Phys. Rev. B* **1999**, 59, 1758.

5. Pascual, J.; Camassel, J.; Mathieu, H. *Phys. Rev. Lett.* **1977**, 39, 1490.

6. Hosaka, N.; Sekiya, T.; Satoko, C.; Kurita, S. *J. Phys. Soc. Jpn.* **1997**, 66, 877.

7. Kang, W. and Hybertsen, M. S. *Phys. Rev. B* **2010**, 82, 085203.

8.Yoshii, K. N.; Ikeda, Y.; Okajima, Y.; Yoneda, Y.; Matsuo, Y. Horibe, S. Mori. *Inorg. Chem.* **2008** , 47, 6493.

9. Kikoin, K.; Fleurov,V. *Phys. Rev. B*, **2006**, 74, 174407-1.

10. Shi, J. B. *Physica C* **1998**, 305, 35.